High-Cycle Fatigue Behaviour of Pure Tantalum under Multiaxial and Variable Amplitude Loadings

MARÉCHAL David[1,a], SAINTIER Nicolas[2,b], PALIN-LUC Thierry[2,c], and NADAL François[1,d]

[1]CEA/Centre d'Études Scientifiques et Techniques d'Aquitaine, 33114 Le Barp, France

[2]Arts et Métiers ParisTech, I2M, CNRS, Université Bordeaux 1, Esplanade des Arts et Métiers, F-33405 Talence, France

[a]david.marechal@u-bordeaux1.fr, [b]nicolas.saintier@ensam.eu, [c]thierry.palin-luc@ensam.eu, [d]francois.nadal@cea.fr

Keywords: High Cycle Fatigue (HCF), Variable Amplitude Loading, Tantalum, Cumulative Damage, Fatigue-Creep Interaction.

Abstract. Due to its specific mechanical properties, tantalum is often used in strength-demanding military applications. High-cycle fatigue (HCF) behaviour of pure tantalum, however, has been rarely reported and the mechanisms at stake to account for deformation under cyclic loadings are still badly understood. This paper aims at better understanding the fatigue behaviour of tantalum and at clarifying the mechanisms of damage formation encountered under such loadings. HCF experiments performed at room temperature on commercially-pure tantalum are presented. Mean stress effects were investigated in the aim of clarifying the interaction between fatigue and creep. Fracture mechanisms were observed to vary from intergranular to transgranular depending on applied stress amplitude and mean stress. Damage mechanisms were investigated under tension and torsion. Results are analyzed in the light of existing fatigue criteria, the limitations of which are discussed. Finally, complex sequential loadings, representative of in-service loadings, were applied to tantalum smooth specimens. The contribution of each loading sequence to the overall damage was quantified and analyzed in terms of linear or non-linear cumulative damage rule.

Introduction

The ability to make accurate fatigue life assessments for materials submitted to variable amplitude loadings is critical to the design of safe components. To this purpose, many models, including those accounting for cumulative damage, have been developed with specific materials, loading sequences and mechanisms in mind, but their generalization remains uncertain. In particular, HCF behaviour of tantalum has been rarely reported and there has been no evaluation of fatigue life models for this material. The scarce published results about HCF behaviour of tantalum show considerable change in fatigue behaviour, depending on loading frequency [1, 2]. While transgranular failure mode was observed under 100 Hz loadings, extended fatigue life was obtained at very high frequencies (20 kHz), together with intergranular crack initiation.

The lack of experimental data does not allow comparing how existing cumulative damage rules perform when applied to tantalum structures submitted to complex loading paths, whether they consist of asymmetric loadings (i.e. stress ratio $R \neq -1$), multiaxial loadings or sequential signals. It is the aim of this paper to introduce carefully-designed experiments for different stress ratios to gain understanding on the HCF deformation mechanisms of tantalum. Both fatigue response and crack initiation mechanisms will be analyzed. Then, variable amplitude sequential loadings will be presented, in view of evaluating existing cumulative damage rules.

Experimental Procedure

Commercially-pure tantalum was provided by Cabot Corporation, as a 6.6 mm thick sheet. The microstructure was fully recrystallized and presented equiaxed grains with average diameter about 80 µm.

Smooth cylindrical fatigue specimens were machined and tested under load control at room temperature using two fatigue testing facilities. The first one was a Zwick vibrophore operating at frequencies around 80 Hz-100 Hz, and delivering sinusoidal signals in tension/compression. The second one was a biaxial electro-dynamic Bose machine, capable of delivering any cyclic signal at frequencies below 50 Hz, both in axial loading (i.e. tension/compression) and torsion. This equipment was also used to generate variable amplitude signals.

The direction of axial loading was always taken parallel to the direction of the last rolling (called RD) of the plate before recrystallization. When torsion was considered, the axis of rotation was also parallel to RD. The specimens were cycled until the appearance of a macro-crack larger than 1 mm on the surface, or until 10^7 cycles if they did not fail. After fatigue testing, the surfaces of failed specimens were observed using a JEOL JSM-840 Scanning Electron Microscope (SEM).

Constant Amplitude Loadings

The S-N curves of pure tantalum represented Fig. 1 showed no effect of the loading frequency in the range [20 Hz, 100 Hz]. Due to confidentiality reasons, all stresses reported here are dimensionless: they have been normalized by the median fatigue strength at 10^7 cycles in tension (R=-1), noted σ_D in the rest of this paper.

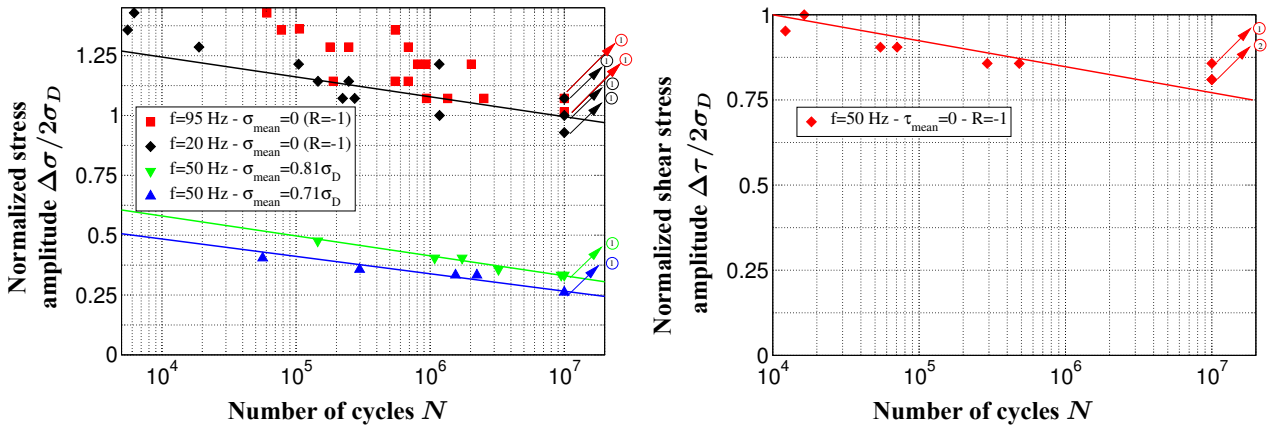

(a) (b)

Fig. 1: S-N curve of tantalum deformed in HCF fatigue, (a) under tension/compression, (b) under symmetric torsion R=-1.

Infra-red thermography was used to analyze plastic energy dissipation, according to the method proposed by Luong [3, 4]. To do so, a single test coupon was submitted to a series of block loadings consisting of 10^4 sinusoidal cycles (20 Hz frequency) with increasing stress amplitudes at each block separated by long (20 min) resting periods enabling return to initial temperature. The temperature on a line localized on the surface of the specimen was monitored with an SC7000 infra-red camera, equipped with a magnifying objective. For each stress amplitude, the temperature variation between the beginning and the end of the 10^4 cycles was calculated. This variation appears in Fig.2 as a function of the applied load level, showing a transition from moderate to much larger self-heating, indicative of a transition from localized to extended plasticity. SEM observations of failed specimens enabled to understand this transition in terms of crack initiation mechanisms: intergranular mode appeared for stress amplitudes below $1.2\sigma_D$, while the fracture was exclusively transgranular for larger stress

amplitudes, suggesting that this transition is a consequence of damage being propagated through grain boundaries. For stress amplitudes close enough to $1.2\sigma_D$, a mixture of intergranular and transgranular initiation could thus be observed, as in micrograph B of Fig. 2(c). In the case of HCF loadings at elevated mean stress ($\sigma_{mean} \geq 0.71\sigma_D$), such transition was also observed for similar value of the maximum stress.

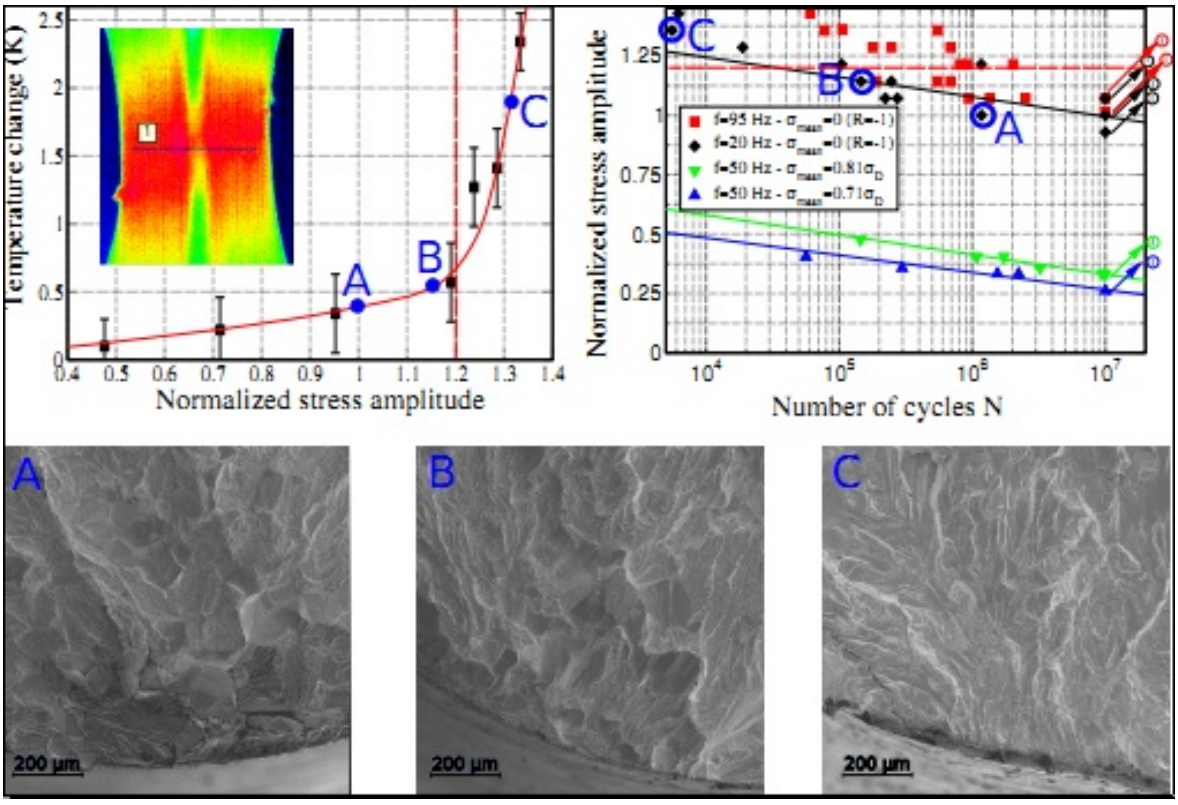

Fig. 2: (a) Temperature change as a function of stress amplitude, indicating two regimes of plasticity. Three conditions of stress amplitudes are highlighted and located on the S-N curve (b). (c) Corresponding fracture surfaces of tantalum specimens loaded in tension (R=-1) showing crack initiation mode varying from intergranular (A) to transgranular (C).

The different stress paths tested here allow comparing different multiaxiality states (i.e. tension and torsion) and different mean stresses. Monotonic tensile tests were also conducted for three strain rates (namely 10^{-4}, 10^{-3} and 10^{-2} s^{-1}), to allow correlating the ultimate tensile strength to the imposed strain rate by a power law. This power law was used to recompute the tensile strength corresponding to the maximum strain rate reached during cyclic loading. It is this value which is plotted as UTS in Fig. 3. Fig. 3(a) shows significant non-linearity in Crossland diagram, suggesting important influence from the hydrostatic stress on fatigue life. Fig. 3(b) shows that the Goodman linear relation linking mean stress and stress amplitude is well-obeyed.

The specimen elongation was recorded for each test conditions, cf. Fig. 4. The evolution of the elongation measured on specimens submitted to elevated mean stresses is characteristic of creep behaviour, and is associated to the formation of a neck. This observation was also confirmed by SEM observations of the fracture surfaces of these specimens (not shown here). Thus, for large values of imposed mean stress, a fatigue-creep interaction appears, which may explain the large deviation from linearity in usual critical plane failure criteria.

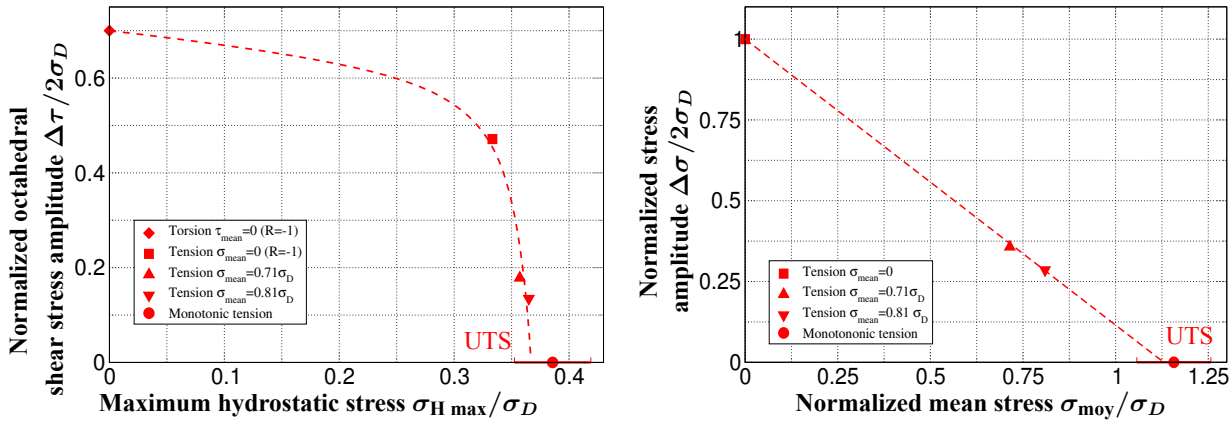

(a) (b)

Fig. 3: Plot of the fatigue strength at 10^7 cycles of pure tantalum upon different tension/torsion paths, (a) in Crossland diagram, (b) in Haigh diagram. UTS refers to the ultimate tensile strength determined in quasi-static monotonic tension with strain rate correction to account for HCF rates.

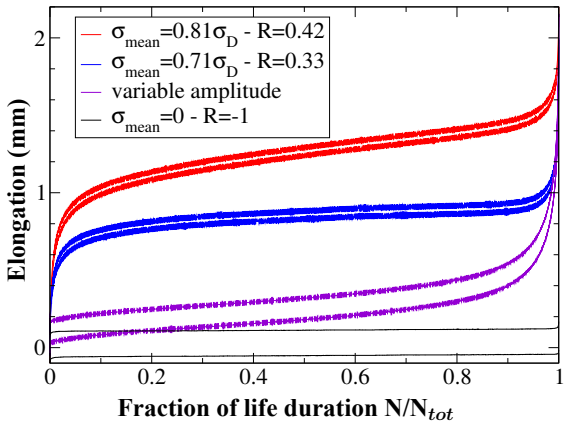

Fig. 4: Evolution of the minimum and maximum elongation plotted towards normalized number of cycles before failure. Except for variable amplitude loadings (see details in Fig. 5(b)), the frequency was imposed to be 50 Hz.

Variable Amplitude Loadings

Variable amplitude loading path consisted of repeated sequences of three sinusoidal blocks, as represented in Fig. 5(a). Blocks 2 and 3 consisted of the same stress levels as described in Fig. 1. The frequency (f_i), time (t_i) and number of cycles (n_i) of each blocks are summarized in Fig. 5(b), together with the number of cycles at failure upon cycling of the block, extrapolated from the data presented in Fig. 1(a). Along these loading sequences, failure of the specimen was observed after 1.3×10^4 sequences. The evolution of elongation, represented in Fig. 4, is characteristic of the loadings with elevated mean stress. Necking was also observed, cf. Fig. 5(c).

Palmgren and Miner proposed that the damage generated by each loading blocks can be added up [5, 6], which results into the numbers of sequences before failure (N_{seq}) to be expressed by Miner's rule:

$$N_{seq} = (n_1/N_1 + n_2/N_2 + n_3/N_3)^{-1} \tag{1}$$

where n_i represent the number of cycles in block i and N_i represent the number of cycles at failure issued from extrapolation of the S-N curves under loading i, cf. Fig. 5.

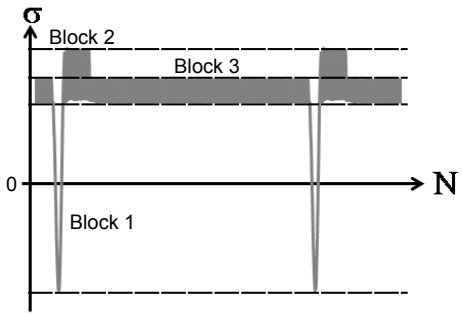

(a)

Quantity	Block 1	Block 2	Block 3
f_i [Hz]	20	100	100
t_i [s]	0.025	0.1	0.89
n_i [cycles]	1	10	89
R_i	-1	0.56	0.73
$\sigma_{mean\ i}$ / σ_D	0	0.81	0.71
N_i [cycles]	3.10^5	2.10^7	10^{10}

(b)

(c)

Fig. 5: (a) Schematic of the sequential tensile loading used in the present study. (b) Loading conditions of each block in the signal represented in (a). (c) Photograph of the specimen submitted to the variable amplitude loading as defined in (b), after failure. The necking area is clearly visible.

Under these hypotheses, the predicted life (2.8×10^5 sequences) was found to be 20 times higher than the one determined experimentally (1.3×10^4 sequences), which shows that Miner's rule is not adapted to evaluate the number of cycles to failure under such variable amplitude loading, most likely due to the high mean stresses of blocks 2 and 3 which caused strong creep damage.

Creep tests are to be implemented to measure damage corresponding to each load level. In the absence of creep data, we used an inverse method consisting in estimating a characteristic time for creep. Creep damage is supposed to follow a law with no exponent (Robinson-Taira law) [7]:

$$D_i = t_i/t_{ci} \tag{2}$$

where t_i is the time spent under stress level i , and t_{ci} is the time to failure under level i. The hypothesis used here is that creep damage and fatigue damage can be added up, as if no coupling existed between these two mechanisms. Under such hypotheses,

$$N_{seq} = (n_1/N_1 + n_2/N_2 + n_3/N_3 + t_2/t_{c2} + t_3/t_{c3})^{-1} \tag{3}$$

Assuming similar critical times for creep under the conditions of block 2 and block 3, an upper boundary of the critical time (called t_c^*) under the mean stress of block 2 ($\sigma_{mean} = 0.81\sigma_D$) can be estimated:

$$t_{c2} < t_c^* = \frac{t_2 + t_3}{N_{seq} - (n_1/N_1 + n_2/N_2 + n_3/N_3)} \simeq 4 \text{ hours} \tag{4}$$

If the experimental value of N_{seq} is used, then we find a critical time for creep under the mean stress of block 2 ($\sigma_{mean} = 0.81\sigma_D$) of no more than 4 hours. However, creep tests operated in such conditions (not detailed here) last much longer than 4 hours. Thus, the cumulative damage appearing in tantalum submitted to asymmetric block loadings (R≠-1) can only be described with a fatigue-creep interaction law. Next step will consist of testing existing models of fatigue-creep interaction, in the light of creep results, in order to determine those that best describe the experimentally-determined fatigue life under current sequential loading. To this regard, the Lemaitre-Chaboche model, which incorporates non-linear interactions and non-linear cumulative effects [7], seems of particular interest.

Summary

High-cycle fatigue behaviour of pure tantalum was investigated. It was found that in the studied range of frequencies (20 Hz-100 Hz), there was no influence of the loading frequency. Along symmetric and asymmetric tension, a transition from transgranular failure to intergranular failure was observed. For elevated mean stresses, a fatigue-creep interaction occurred, which resulted in significant fatigue life

reduction. This fatigue-creep interaction was reflected in blatant non-linearity in Crossland diagram. Variable amplitude loadings alternating blocks at different mean stresses also revealed an important creep regime. In these loadings, the classical Miner's rule does not apear suitable, even if creep damage contributions are added to the usual formulation. These results confirm the important interaction between fatigue and creep in tantalum.

References

[1] M. Papakyriakou, H. Mayer, C. Pypen, H. Plenk Jr, S. Stanzl-Tschegg: Mat. Sci. Eng. Vol. A308 (2001), p. 143

[2] M. Papakyriakou, H. Mayer, H. Plenk Jr, S. Stanzl-Tschegg: Mat. Sci. Eng. Vol. A325 (2002), p. 520

[3] M.P. Luong: Nucl. Eng. Des. Vol. 158 (1995), p. 363

[4] G. La Rosa, A. Risitano: Int. J. Fat. Vol. 22 (2000), p. 65

[5] A. Palmgren: Verfahrenstechinik Vol. 68 (1924), p. 339

[6] M. Miner: J. Appl. Mech. ASME Vol. 67 (1945), p. 159

[7] J. Lemaitre, J-L. Chaboche: Mécanique des matériaux solides, edited by Dunod Paris (2001)